

PAPER • OPEN ACCESS

Evidence for the decays of $\Lambda_c^+ \rightarrow \Sigma^+ \eta$ and $\Sigma^+ \eta'$ ^{*}

To cite this article: M. Ablikim *et al* 2019 *Chinese Phys. C* **43** 083002

Recent citations

- [Charmed baryon weak decays with vector mesons](#)
C. Q. Geng *et al*

View the [article online](#) for updates and enhancements.

Evidence for the decays of $\Lambda_c^+ \rightarrow \Sigma^+ \eta$ and $\Sigma^+ \eta'^*$

M. Ablikim(麦迪娜)¹ M. N. Achasov^{10,d} S. Ahmed¹⁵ M. Albrecht⁴ M. Alekseev^{56A,56C} A. Amoroso^{56A,56C}
 F. F. An(安芬芬)¹ Q. An(安琪)^{43,53} Y. Bai(白羽)⁴² O. Bakina²⁷ R. Baldini Ferroli^{23A} Y. Ban(班勇)³⁵
 K. Begzsuren²⁵ D. W. Bennett²² J. V. Bennett⁵ N. Berger²⁶ M. Bertani^{23A} D. Bettoni^{24A} F. Bianchi^{56A,56C}
 I. Boyko²⁷ R. A. Briere⁵ H. Cai(蔡浩)⁵⁸ X. Cai(蔡啸)^{1,43} O. Cakir^{46A} A. Calcaterra^{23A} G. F. Cao(曹国富)^{1,47}
 S. A. Cetin^{46B} J. Chai^{56C} J. F. Chang(常劲帆)^{1,43} W. L. Chang^{1,47} G. Chelkov^{27,b,c} G. Chen(陈刚)¹
 H. S. Chen(陈和生)^{1,47} J. C. Chen(陈江川)¹ M. L. Chen(陈玛丽)^{1,43} P. L. Chen(陈平亮)⁵⁴ S. J. Chen(陈申见)³³
 Y. B. Chen(陈元柏)^{1,43} W. Cheng(成伟帅)^{56C} G. Cibinetto^{24A} F. Cossio^{56C} H. L. Dai(代洪亮)^{1,43}
 J. P. Dai(代建平)^{38,h} A. Dbeysi¹⁵ D. Dedovich²⁷ Z. Y. Deng(邓子艳)¹ A. Denig²⁶ I. Denysenko²⁷
 M. Destefanis^{56A,56C} F. De Mori^{56A,56C} Y. Ding(丁勇)³¹ C. Dong(董超)³⁴ J. Dong(董静)^{1,43}
 L. Y. Dong(董燎原)^{1,47} M. Y. Dong(董明义)¹ Z. L. Dou(豆正磊)³³ S. X. Du(杜书先)⁶¹ P. F. Duan(段鹏飞)¹
 J. Z. Fan(范荆州)⁴⁵ J. Fang(方建)^{1,43} S. S. Fang(房双世)^{1,47} Y. Fang(方易)¹ R. Farinelli^{24A,24B} L. Fava^{56B,56C}
 S. Fegan²⁶ F. Feldbauer⁴ G. Felici^{23A} C. Q. Feng(封常青)^{43,53} M. Fritsch⁴ C. D. Fu(傅成栋)¹ Y. Fu(付颖)¹
 Q. Gao(高清)¹ X. L. Gao(高鑫磊)^{43,53} Y. Gao(高原宁)⁴⁵ Y. G. Gao(高勇贵)⁶ Z. Gao(高榛)^{43,53} B. Garillon²⁶
 I. Garzia^{24A} A. Gilman⁵⁰ K. Goetzen¹¹ L. Gong(龚丽)³⁴ W. X. Gong(龚文煊)^{1,43} W. Gradl²⁶ M. Greco^{56A,56C}
 L. M. Gu(谷立民)³³ M. H. Gu(顾曼皓)^{1,43} Y. T. Gu(顾运厅)¹³ A. Q. Guo(郭爱强)¹ L. B. Guo(郭立波)³²
 R. P. Guo(郭如盼)^{1,47} Y. P. Guo(郭玉萍)²⁶ A. Guskov²⁷ Z. Haddadi²⁹ S. Han(韩爽)⁵⁸ X. Q. Hao(郝喜庆)¹⁶
 F. A. Harris⁴⁸ K. L. He(何康林)^{1,47} F. H. Heinrichs⁴ T. Held⁴ Y. K. Heng(衡月昆)¹ Z. L. Hou(侯治龙)¹
 H. M. Hu(胡海明)^{1,47} J. F. Hu(胡继峰)^{38,h} T. Hu(胡涛)¹ Y. Hu(胡誉)¹ G. S. Huang(黄光顺)^{43,53}
 J. S. Huang(黄金书)¹⁶ X. T. Huang(黄性涛)³⁷ X. Z. Huang(黄晓忠)³³ Z. L. Huang(黄智玲)³¹
 T. Hussain⁵⁵ N. Hüskens⁵¹ W. Ikegami Andersson⁵⁷ M. Irshad^{43,53} Q. Ji(纪全)¹ Q. P. Ji(姬清平)¹⁶
 X. B. Ji(季晓斌)^{1,47} X. L. Ji(季筱璐)^{1,43} X. S. Jiang(江晓山)¹ X. Y. Jiang(蒋兴雨)³⁴ J. B. Jiao(焦健斌)³⁷
 Z. Jiao(焦铮)¹⁸ D. P. Jin(金大鹏)¹ S. Jin(金山)³³ Y. Jin(金毅)⁴⁹ T. Johansson⁵⁷ A. Julin⁵⁰
 N. Kalantar-Nayestanaki²⁹ X. S. Kang(康晓坤)³⁴ M. Kavatsyuk²⁹ B. C. Ke(柯百谦)¹ I. K. Keshk⁴ T. Khan^{43,53}
 A. Khoukaz⁵¹ P. Kiese²⁶ R. Kiuchi¹ R. Kliemt¹¹ L. Koch²⁸ O. B. Kolcu^{46B,f} B. Kopf⁴ M. Kornicer⁴⁸
 M. Kuemmel⁴ M. Kuessner⁴ A. Kupsc⁵⁷ M. Kurth¹ W. Kühn²⁸ J. S. Lange²⁸ P. Larin¹⁵ L. Lavezzi^{1,56C}
 S. Leiber⁴ H. Leithoff²⁶ C. Li(李翠)⁵⁷ Cheng Li(李澄)^{43,53} D. M. Li(李德民)⁶¹ F. Li(李飞)^{1,43}
 F. Y. Li(李峰云)³⁵ G. Li(李刚)¹ H. B. Li(李海波)^{1,47} H. J. Li(李惠静)^{1,47} J. C. Li(李家才)¹
 J. W. Li(李井文)⁴¹ Ke Li(李科)¹ Lei Li(李蕾)³ P. L. Li(李佩莲)^{43,53} P. R. Li(李培荣)^{7,47}
 Q. Y. Li(李启云)³⁷ T. Li(李腾)³⁷ W. D. Li(李卫东)^{1,47} W. G. Li(李卫国)¹ X. L. Li(李晓玲)³⁷
 X. N. Li(李小男)^{1,43} X. Q. Li(李学潜)³⁴ Z. B. Li(李志兵)⁴⁴ H. Liang(梁昊)^{43,53} Y. F. Liang(梁勇飞)⁴⁰
 Y. T. Liang(梁羽铁)²⁸ G. R. Liao(廖广睿)¹² L. Z. Liao(廖龙洲)^{1,47} J. Libby²¹ C. X. Lin(林创新)⁴⁴
 D. X. Lin(林德旭)¹⁵ B. Liu(刘冰)^{38,h} B. J. Liu(刘北江)¹ C. X. Liu(刘春秀)¹ D. Liu(刘栋)^{43,53}

Received 22 November 2018, Revised 16 February 2019, Published online 3 July 2019

* Supported in part by National Key Basic Research Program of China (2015CB856700); National Natural Science Foundation of China (NSFC)(11235011, 11275266, 11335008, 11425524, 11625523, 11635010); the Chinese Academy of Sciences (CAS) Large-Scale Scientific Facility Program; the CAS Center for Excellence in Particle Physics (CCEPP); Joint Large-Scale Scientific Facility Funds of the NSFC and CAS (U1332201, U1532257, U1532258); CAS (KJCX2-YW-N29, KJCX2-YW-N45, QYZDJ-SSW-SLH003); 100 Talents Program of CAS; National 1000 Talents Program of China; INPAC and Shanghai Key Laboratory for Particle Physics and Cosmology; German Research Foundation DFG (Collaborative Research Center CRC 1044, FOR 2359); Istituto Nazionale di Fisica Nucleare, Italy; Koninklijke Nederlandse Akademie van Wetenschappen (KNAW) (530-4CDP03); Ministry of Development of Turkey (DPT2006K-120470); National Science and Technology fund; The Swedish Research Council; U. S. Department of Energy under (DE-FG02-05ER41374, DE-SC-0010118, DE-SC-0010504, DE-SC-0012069); University of Groningen (RuG) and the Helmholtzzentrum fuer Schwerionenforschung GmbH (GSI), Darmstadt; WCU Program of National Research Foundation of Korea (R32-2008-000-10155-0)

 Content from this work may be used under the terms of the Creative Commons Attribution 3.0 licence. Any further distribution of this work must maintain attribution to the author(s) and the title of the work, journal citation and DOI. Article funded by SCOAP3 and published under licence by Chinese Physical Society and the Institute of High Energy Physics of the Chinese Academy of Sciences and the Institute of Modern Physics of the Chinese Academy of Sciences and IOP Publishing Ltd

- D. Y. Liu(刘殿宇)^{38,h} F. H. Liu(刘福虎)³⁹ Fang Liu(刘芳)¹ Feng Liu(刘峰)⁶ H. B. Liu(刘宏邦)¹³
H. L. Liu(刘恒君)⁴² H. M. Liu(刘怀民)^{1,47} Huanhuan Liu(刘欢欢)¹ Huihui Liu(刘汇慧)¹⁷ J. B. Liu(刘建北)^{43,53}
J. Y. Liu(刘晶译)^{1,47} K. Liu(刘凯)⁴⁵ K. Y. Liu(刘魁勇)³¹ Ke Liu(刘珂)⁶ Q. Liu(刘倩)⁴⁷
S. B. Liu(刘树彬)^{43,53} X. Liu(刘翔)³⁰ Y. B. Liu(刘玉斌)³⁴ Z. A. Liu(刘振安)¹ Zhiqing Liu(刘智青)²⁶
Y. F. Long(龙云飞)³⁵ X. C. Lou(娄辛丑)¹ H. J. Lu(吕海江)¹⁸ J. D. Lu(陆嘉达)^{1,47} J. G. Lu(吕军光)^{1,43}
Y. Lu(卢宇)¹ Y. P. Lu(卢云鹏)^{1,43} C. L. Luo(罗成林)³² M. X. Luo(罗民兴)⁶⁰ T. Luo(罗涛)^{9,j}
X. L. Luo(罗小兰)^{1,43} S. Lusso^{56C} X. R. Lyu(吕晓睿)⁴⁷ F. C. Ma(马凤才)³¹ H. L. Ma(马海龙)¹
L. L. Ma(马连良)³⁷ M. M. Ma(马明明)^{1,47} Q. M. Ma(马秋梅)¹ X. N. Ma(马旭宁)³⁴ X. X. Ma(马新鑫)^{1,47}
X. Y. Ma(马骁妍)^{1,43} Y. M. Ma(马玉明)³⁷ F. E. Maas¹⁵ M. Maggiora^{56A,56C} S. Maldaner²⁶ Q. A. Malik⁵⁵
A. Mangoni^{23B} Y. J. Mao(冒亚军)³⁵ Z. P. Mao(毛泽普)¹ S. Marcello^{56A,56C} Z. X. Meng(孟召霞)⁴⁹
J. G. Messchendorp²⁹ G. Mezzadri^{24A} J. Min(闵建)^{1,43} T. J. Min(闵天觉)³³ R. E. Mitchell²²
X. H. Mo(莫晓虎)¹ Y. J. Mo(莫玉俊)⁶ C. Morales Morales¹⁵ N. Yu. Muchnoi^{10,d} H. Muramatsu⁵⁰ A. Mustafa⁴
S. Nakhoul^{11,g} Y. Nefedov²⁷ F. Nerling^{11,g} I. B. Nikolaev^{10,d} Z. Ning(宁哲)^{1,43} S. Nisar^{8,l}
S. L. Niu(牛顺利)^{1,43} S. L. Olsen(马鹏)^{36,k} Q. Ouyang(欧阳群)¹ S. Pacetti^{23B} Y. Pan(潘越)^{43,53}
M. Papenbrock⁵⁷ P. Patteri^{23A} M. Pelizaeus⁴ J. Pellegrino^{56A,56C} H. P. Peng(彭海平)^{43,53} K. Peters^{11,g}
J. Pettersson⁵⁷ J. L. Ping(平加伦)³² R. G. Ping(平荣刚)^{1,47} A. Pitka⁴ R. Poling⁵⁰ V. Prasad^{43,53}
H. R. Qi(漆红荣)² M. Qi(祁鸣)³³ T. Y. Qi(齐天钰)² S. Qian(钱森)^{1,43} C. F. Qiao(乔从丰)⁴⁷ N. Qin(覃拈)⁵⁸
X. S. Qin⁴ Z. H. Qin(秦中华)^{1,43} J. F. Qiu(邱进发)¹ S. Q. Qu(屈三强)³⁴ K. H. Rashid^{55,i} C. F. Redmer²⁶
M. Richter⁴ M. Ripka²⁶ A. Rivetti^{56C} M. Rolo^{56C} G. Rong(荣刚)^{1,47} Ch. Rosner¹⁵ M. Rump⁵¹
A. Sarantsev^{27,e} M. Savrié^{24B} K. Schoenning⁵⁷ W. Shan(单葳)¹⁹ X. Y. Shan(单心钰)^{43,53} M. Shao(邵明)^{43,53}
C. P. Shen(沈成平)² P. X. Shen(沈培迅)³⁴ X. Y. Shen(沈肖雁)^{1,47} H. Y. Sheng(盛华义)¹ X. Shi(史欣)^{1,43}
J. J. Song(宋娇娇)³⁷ W. M. Song³⁷ X. Y. Song(宋欣颖)¹ S. Sosio^{56A,56C} C. Sowa⁴ S. Spataro^{56A,56C}
G. X. Sun(孙功星)¹ J. F. Sun(孙俊峰)¹⁶ L. Sun(孙亮)⁵⁸ S. S. Sun(孙胜森)^{1,47} X. H. Sun(孙新华)¹
Y. J. Sun(孙勇杰)^{43,53} Y. K. Sun(孙艳坤)^{43,53} Y. Z. Sun(孙永昭)¹ Z. J. Sun(孙志嘉)^{1,43} Z. T. Sun(孙振田)¹
Y. T. Tan(谭雅星)^{43,53} C. J. Tang(唐昌建)⁴⁰ G. Y. Tang(唐光毅)¹ X. Tang(唐晓)¹ I. Tapan^{46c} M. Tiemens²⁹
B. Tsednee²⁵ I. Uman^{46D} B. Wang(王斌)¹ B. L. Wang(王滨龙)⁴⁷ C. W. Wang(王成伟)³³
D. Y. Wang(王大勇)³⁵ Dan Wang(王丹)⁴⁷ K. Wang(王科)^{1,43} L. L. Wang(王亮亮)¹ L. S. Wang(王灵淑)¹
M. Wang(王萌)³⁷ Meng Wang(王蒙)^{1,47} P. Wang(王平)¹ P. L. Wang(王佩良)¹ W. P. Wang(王维平)^{43,53}
X. F. Wang(王雄飞)¹ Y. Wang(王越)^{43,53} Y. F. Wang(王贻芳)¹ Z. Wang(王铮)^{1,43} Z. G. Wang(王志刚)^{1,43}
Z. Y. Wang(王至勇)¹ Zongyuan Wang(王宗源)^{1,47} T. Weber⁴ D. H. Wei(魏代会)¹² P. Weidenkaff²⁶
S. P. Wen(文硕频)¹ U. Wiedner⁴ M. Wolke⁵⁷ L. H. Wu(伍灵慧)¹ L. J. Wu(吴连近)^{1,47} Z. Wu(吴智)^{1,43}
L. Xia(夏磊)^{43,53} X. Xia³⁷ Y. Xia(夏宇)²⁰ D. Xiao(肖栋)¹ Y. J. Xiao(肖言佳)^{1,47} Z. J. Xiao(肖振军)³²
Y. G. Xie(谢宇广)^{1,43} Y. H. Xie(谢跃红)⁶ X. A. Xiong(熊习安)^{1,47} Q. L. Xiu(修青磊)^{1,43} G. F. Xu(许国发)¹
J. J. Xu(徐静静)^{1,47} L. Xu(徐雷)¹ Q. J. Xu(徐庆君)¹⁴ Q. N. Xu(徐庆年)⁴⁷ X. P. Xu(徐新平)⁴¹ F. Yan(严芳)⁵⁴
L. Yan(严亮)^{56A,56C} W. B. Yan(鄢文标)^{43,53} W. C. Yan(闫文成)² Y. H. Yan(颜永红)²⁰ H. J. Yang(杨海军)^{38,h}
H. X. Yang(杨洪勋)¹ L. Yang(杨柳)⁵⁸ R. X. Yang^{43,53} S. L. Yang(杨双莉)^{1,47} Y. H. Yang(杨友华)³³
Y. X. Yang(杨永栩)¹² Yifan Yang(杨翊凡)^{1,47} Z. Q. Yang(杨子倩)²⁰ M. Ye(叶梅)^{1,43} M. H. Ye(叶铭汉)⁷
J. H. Yin(殷俊昊)¹ Z. Y. You(尤郑昀)⁴⁴ B. X. Yu(俞伯祥)¹ C. X. Yu(喻纯旭)³⁴ J. S. Yu(俞洁晟)²⁰
C. Z. Yuan(苑长征)^{1,47} Y. Yuan(袁野)¹ A. Yuncu^{46B,a} A. A. Zafar⁵⁵ Y. Zeng(曾云)²⁰
B. X. Zhang(张丙新)¹ B. Y. Zhang(张炳云)^{1,43} C. C. Zhang(张长春)¹ D. H. Zhang(张达华)¹
H. H. Zhang(张宏浩)⁴⁴ H. Y. Zhang(章红宇)^{1,43} J. Zhang(张晋)^{1,47} J. L. Zhang(张杰磊)⁵⁹ J. Q. Zhang⁴
J. W. Zhang(张家文)¹ J. Y. Zhang(张建勇)¹ J. Z. Zhang(张景芝)^{1,47} K. Zhang(张坤)^{1,47} L. Zhang(张磊)⁴⁵
S. F. Zhang(张思凡)³³ T. J. Zhang(张天骄)^{38,h} X. Y. Zhang(张学尧)³⁷ Y. Zhang(张言)^{43,53}
Y. H. Zhang(张银鸿)^{1,43} Y. T. Zhang(张亚腾)^{43,53} Yang Zhang(张洋)¹ Yao Zhang(张瑶)¹ Yu Zhang(张宇)⁴⁷
Z. H. Zhang(张正好)⁶ Z. P. Zhang(张子平)⁵³ Z. Y. Zhang(张振宇)⁵⁸ G. Zhao(赵光)¹ J. W. Zhao(赵京伟)^{1,43}
J. Y. Zhao(赵静宜)^{1,47} J. Z. Zhao(赵京周)^{1,43} Lei Zhao(赵雷)^{43,53} Ling Zhao(赵玲)¹ M. G. Zhao(赵明刚)³⁴

Q. Zhao(赵强)¹ S. J. Zhao(赵书俊)⁶¹ T. C. Zhao(赵天池)¹ Y. B. Zhao(赵豫斌)^{1,43} Z. G. Zhao(赵政国)^{43,53}
 A. Zhemchugov^{27,b} B. Zheng(郑波)⁵⁴ J. P. Zheng(郑建平)^{1,43} W. J. Zheng(郑文静)³⁷ Y. H. Zheng(郑阳恒)⁴⁷
 B. Zhong(钟彬)³² L. Zhou(周莉)^{1,43} Q. Zhou(周巧)^{1,47} X. Zhou(周详)⁵⁸ X. K. Zhou(周晓康)^{43,53}
 X. R. Zhou(周小蓉)^{43,53} X. Y. Zhou(周兴玉)¹ Xiaoyu Zhou(周晓宇)²⁰ Xu Zhou(周旭)²⁰ A. N. Zhu(朱傲男)^{1,47}
 J. Zhu(朱江)³⁴ J. Zhu(朱江)⁴⁴ K. Zhu(朱凯)¹ K. J. Zhu(朱科军)¹ S. Zhu(朱帅)¹ S. H. Zhu(朱世海)⁵²
 X. L. Zhu(朱相雷)⁴⁵ Y. C. Zhu(朱莹春)^{43,53} Y. S. Zhu(朱永生)^{1,47} Z. A. Zhu(朱自安)^{1,47} J. Zhuang(庄建)^{1,43}
 B. S. Zou(邹冰松)¹ J. H. Zou(邹佳恒)¹
 (BESIII Collaboration)

¹Institute of High Energy Physics, Beijing 100049, People's Republic of China

²Beihang University, Beijing 100191, People's Republic of China

³Beijing Institute of Petrochemical Technology, Beijing 102617, People's Republic of China

⁴Bochum Ruhr-University, D-44780 Bochum, Germany

⁵Carnegie Mellon University, Pittsburgh, Pennsylvania 15213, USA

⁶Central China Normal University, Wuhan 430079, People's Republic of China

⁷China Center of Advanced Science and Technology, Beijing 100190, People's Republic of China

⁸COMSATS Institute of Information Technology, Lahore, Defence Road, Off Raiwind Road, 54000 Lahore, Pakistan

⁹Fudan University, Shanghai 200443, People's Republic of China

¹⁰G.I. Budker Institute of Nuclear Physics SB RAS (BINP), Novosibirsk 630090, Russia

¹¹GSI Helmholtzcentre for Heavy Ion Research GmbH, D-64291 Darmstadt, Germany

¹²Guangxi Normal University, Guilin 541004, People's Republic of China

¹³Guangxi University, Nanning 530004, People's Republic of China

¹⁴Hangzhou Normal University, Hangzhou 310036, People's Republic of China

¹⁵Helmholtz Institute Mainz, Johann-Joachim-Becher-Weg 45, D-55099 Mainz, Germany

¹⁶Henan Normal University, Xinxiang 453007, People's Republic of China

¹⁷Henan University of Science and Technology, Luoyang 471003, People's Republic of China

¹⁸Huangshan College, Huangshan 245000, People's Republic of China

¹⁹Hunan Normal University, Changsha 410081, People's Republic of China

²⁰Hunan University, Changsha 410082, People's Republic of China

²¹Indian Institute of Technology Madras, Chennai 600036, India

²²Indiana University, Bloomington, Indiana 47405, USA

²³(A)INFN Laboratori Nazionali di Frascati, I-00044, Frascati, Italy; (B)INFN and University of Perugia, I-06100, Perugia, Italy

²⁴(A)INFN Sezione di Ferrara, I-44122, Ferrara, Italy; (B)University of Ferrara, I-44122, Ferrara, Italy

²⁵Institute of Physics and Technology, Peace Ave. 54B, Ulaanbaatar 13330, Mongolia

²⁶Johannes Gutenberg University of Mainz, Johann-Joachim-Becher-Weg 45, D-55099 Mainz, Germany

²⁷Joint Institute for Nuclear Research, 141980 Dubna, Moscow region, Russia

²⁸Justus-Liebig-Universitaet Giessen, II. Physikalisches Institut, Heinrich-Buff-Ring 16, D-35392 Giessen, Germany

²⁹KVI-CART, University of Groningen, NL-9747 AA Groningen, The Netherlands

³⁰Lanzhou University, Lanzhou 730000, People's Republic of China

³¹Liaoning University, Shenyang 110036, People's Republic of China

³²Nanjing Normal University, Nanjing 210023, People's Republic of China

³³Nanjing University, Nanjing 210093, People's Republic of China

³⁴Nankai University, Tianjin 300071, People's Republic of China

³⁵Peking University, Beijing 100871, People's Republic of China

³⁶Seoul National University, Seoul, 151-747 Korea

³⁷Shandong University, Jinan 250100, People's Republic of China

³⁸Shanghai Jiao Tong University, Shanghai 200240, People's Republic of China

³⁹Shanxi University, Taiyuan 030006, People's Republic of China

⁴⁰Sichuan University, Chengdu 610064, People's Republic of China

⁴¹Soochow University, Suzhou 215006, People's Republic of China

⁴²Southeast University, Nanjing 211100, People's Republic of China

⁴³State Key Laboratory of Particle Detection and Electronics, Beijing 100049, Hefei 230026, People's Republic of China

⁴⁴Sun Yat-Sen University, Guangzhou 510275, People's Republic of China

⁴⁵Tsinghua University, Beijing 100084, People's Republic of China

⁴⁶(A)Ankara University, 06100 Tandoğan, Ankara, Turkey; (B)İstanbul Bilgi University, 34060 Eyyüp, İstanbul, Turkey; (C)Uludag University, 16059 Bursa, Turkey; (D)Near East University, Nicosia, North Cyprus, Mersin 10, Turkey

⁴⁷University of Chinese Academy of Sciences, Beijing 100049, People's Republic of China

⁴⁸University of Hawaii, Honolulu, Hawaii 96822, USA

⁴⁹University of Jinan, Jinan 250022, People's Republic of China

⁵⁰University of Minnesota, Minneapolis, Minnesota 55455, USA

⁵¹University of Muenster, Wilhelm-Klemm-Str. 9, 48149 Muenster, Germany

⁵²University of Science and Technology Liaoning, Anshan 114051, People's Republic of China

⁵³University of Science and Technology of China, Hefei 230026, People's Republic of China

⁵⁴University of South China, Hengyang 421001, People's Republic of China

⁵⁵University of the Punjab, Lahore-54590, Pakistan

⁵⁶(A)University of Turin, I-10125, Turin, Italy; (B)University of Eastern Piedmont, I-15121, Alessandria, Italy; (C)INFN, I-10125, Turin, Italy⁵⁷Uppsala University, Box 516, SE-75120 Uppsala, Sweden⁵⁸Wuhan University, Wuhan 430072, People's Republic of China⁵⁹Xinyang Normal University, Xinyang 464000, People's Republic of China⁶⁰Zhejiang University, Hangzhou 310027, People's Republic of China⁶¹Zhengzhou University, Zhengzhou 450001, People's Republic of China^aAlso at Bogazici University, 34342 Istanbul, Turkey^bAlso at the Moscow Institute of Physics and Technology, Moscow 141700, Russia^cAlso at the Functional Electronics Laboratory, Tomsk State University, Tomsk, 634050, Russia^dAlso at the Novosibirsk State University, Novosibirsk, 630090, Russia^eAlso at the NRC "Kurchatov Institute", PNPI, 188300, Gatchina, Russia^fAlso at Istanbul Arel University, 34295 Istanbul, Turkey^gAlso at Goethe University Frankfurt, 60323 Frankfurt am Main, Germany^hAlso at Key Laboratory for Particle Physics, Astrophysics and Cosmology, Ministry of Education; Shanghai Key Laboratory for Particle Physics and Cosmology; Institute of Nuclear and Particle Physics, Shanghai 200240, People's Republic of ChinaⁱAlso at Government College Women University, Sialkot - 51310, Punjab, Pakistan.^jAlso at Key Laboratory of Nuclear Physics and Ion-beam Application (MOE) and Institute of Modern Physics, Fudan University, Shanghai 200443, People's Republic of China^kCurrently at: Center for Underground Physics, Institute for Basic Science, Daejeon 34126, Korea^lAlso at Harvard University, Department of Physics, Cambridge, MA, 02138, USA

Abstract: We study the hadronic decays of Λ_c^+ to the final states $\Sigma^+\eta$ and $\Sigma^+\eta'$, using an e^+e^- annihilation data sample of 567 pb^{-1} taken at a center-of-mass energy of 4.6 GeV with the BESIII detector at the BEPCII collider. We find evidence for the decays $\Lambda_c^+ \rightarrow \Sigma^+\eta$ and $\Sigma^+\eta'$ with statistical significance of 2.5σ and 3.2σ , respectively. Normalizing to the reference decays $\Lambda_c^+ \rightarrow \Sigma^+\pi^0$ and $\Sigma^+\omega$, we obtain the ratios of the branching fractions $\frac{\mathcal{B}(\Lambda_c^+ \rightarrow \Sigma^+\eta)}{\mathcal{B}(\Lambda_c^+ \rightarrow \Sigma^+\pi^0)}$ and $\frac{\mathcal{B}(\Lambda_c^+ \rightarrow \Sigma^+\eta')}{\mathcal{B}(\Lambda_c^+ \rightarrow \Sigma^+\omega)}$ to be $0.35 \pm 0.16 \pm 0.02$ and $0.86 \pm 0.34 \pm 0.04$, respectively. The upper limits at the 90% confidence level are set to be $\frac{\mathcal{B}(\Lambda_c^+ \rightarrow \Sigma^+\eta)}{\mathcal{B}(\Lambda_c^+ \rightarrow \Sigma^+\pi^0)} < 0.58$ and $\frac{\mathcal{B}(\Lambda_c^+ \rightarrow \Sigma^+\eta')}{\mathcal{B}(\Lambda_c^+ \rightarrow \Sigma^+\omega)} < 1.2$. Using BESIII measurements of the branching fractions of the reference decays, we determine $\mathcal{B}(\Lambda_c^+ \rightarrow \Sigma^+\eta) = (0.41 \pm 0.19 \pm 0.05)\%$ ($< 0.68\%$) and $\mathcal{B}(\Lambda_c^+ \rightarrow \Sigma^+\eta') = (1.34 \pm 0.53 \pm 0.19)\%$ ($< 1.9\%$). Here, the first uncertainties are statistical and the second systematic. The obtained branching fraction of $\Lambda_c^+ \rightarrow \Sigma^+\eta$ is consistent with the previous measurement, and the branching fraction of $\Lambda_c^+ \rightarrow \Sigma^+\eta'$ is measured for the first time.

Keywords: charmed baryon, Λ_c^+ decays, branching fractions

PACS: 13.66.Bc, 14.20.Lq, 13.30.Eg **DOI:** 10.1088/1674-1137/43/8/083002

1 Introduction

Nonleptonic decays of charmed baryons offer excellent opportunities for testing different theoretical approaches to describe the complicated dynamics of heavy-light baryons, including the current algebra approach [1], the factorization scheme, the pole model technique [2-4], the relativistic quark model [5, 6] and the quark-diagram scheme [7]. Contrary to the significant progress made in the studies of heavy meson decays, the progress in both theoretical and experimental studies of heavy baryon decays is relatively sparse. The Λ_c^+ was first observed at the Mark II experiment in 1979 [8], but only about 60% of its decays have been accounted for so far and the rest still remain unknown [9].

The two-body Cabibbo-favored (CF) decay of the Λ_c^+ to an octet baryon and a pseudoscalar meson, $\Lambda_c^+ \rightarrow$

$B\left(\frac{1}{2}^+\right)P$, is one of the simplest hadronic channels to be treated theoretically [10], and measurements of the branching fractions (BFs) can be used to calibrate different theoretical approaches. Recently, BESIII has studied twelve CF Λ_c^+ decay modes, among which the absolute BFs for $B\left(\frac{1}{2}^+\right)P$ decays $\Lambda_c^+ \rightarrow pK_S^0$, $\Lambda\pi^+$, $\Sigma^0\pi^+$ and $\Sigma^+\pi^0$ are significantly improved in precision [11]. However, other CF modes are only known with poor precision, or even have not been explored yet.

The CF decays $\Lambda_c^+ \rightarrow \Sigma^+\eta$ and $\Sigma^+\eta'$ proceed entirely through nonfactorizable internal W -emission and W -exchange diagrams, as shown in Fig. 1, and are particularly interesting. Unlike the case for charmed meson decays, these nonfactorizable decays are free from color and helicity suppressions and are quite sizable. Theoretical predictions on these nonfactorizable effects are not reliable,

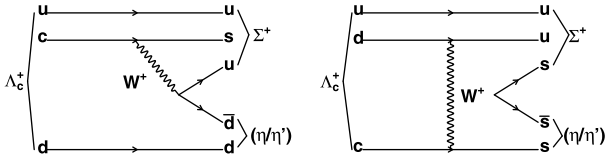


Fig. 1. Representative tree level diagrams of decays of $\Lambda_c^+ \rightarrow \Sigma^+\eta$ and $\Lambda_c^+ \rightarrow \Sigma^+\eta'$.

however, resulting in very large variations of the predicted BFs, e.g., $\mathcal{B}(\Lambda_c^+ \rightarrow \Sigma^+\eta) = (0.11 - 0.94)\%$, and $\mathcal{B}(\Lambda_c^+ \rightarrow \Sigma^+\eta') = (0.1 - 1.28)\%$ [3-6]. On the experimental side, only evidence for $\Lambda_c^+ \rightarrow \Sigma^+\eta$ has been reported by CLEO [12] with a BF of $(0.70 \pm 0.23)\%$, and the channel $\Lambda_c^+ \rightarrow \Sigma^+\eta'$ is yet to be observed. Hence, further experimental studies of these two decay modes are essential for testing different theoretical models and for a better understanding of the Λ_c^+ CF decays.

In this work, BFs for $\Lambda_c^+ \rightarrow \Sigma^+\eta$ and $\Sigma^+\eta'$ are measured with respect to the CF modes $\Lambda_c^+ \rightarrow \Sigma^+\pi^0$ and $\Sigma^+\omega$, respectively, by analyzing 567 pb^{-1} [13] data taken at $\sqrt{s} = 4.6 \text{ GeV}$ [14] with the BESIII detector at the BEPCII collider. Throughout this paper, charge-conjugate modes are always implied.

2 BESIII detector

The BESIII detector has a geometrical acceptance of 93% of 4π and consists of the following main components: 1) a small-celled, helium-based main draft chamber (MDC) with 43 layers. The average single wire resolution is $135 \mu\text{m}$, and the momentum resolution for 1 GeV/c charged particles in a 1 T magnetic field is 0.5%; 2) a Time-Of-Flight system (TOF) for particle identification composed of a barrel part made of two layers with 88 pieces of 5 cm thick, 2.4 m long plastic scintillator in each layer, and two end-caps each with 96 fan-shaped, 5 cm thick, plastic scintillators. The time resolution is 80 ps in the barrel, and 110 ps in the endcaps, corresponding to a 2σ K/ π separation for momenta up to about 1.0 GeV/c; 3) an electromagnetic calorimeter (EMC) made of 6240 CsI (Tl) crystals arranged in a cylindrical shape (barrel) plus two end-caps. For 1.0 GeV photons, the energy resolution is 2.5% in the barrel and 5% in the end-caps, and the position resolution is 6 mm in the barrel and 9 mm in the end-caps; 4) a muon chamber system (MUC) made of Resistive Plate Chambers (RPC) arranged in 9 layers in the barrel and 8 layers in the endcaps and incorporated in the return iron of the superconducting magnet. The position resolution is about 2 cm. More details about the design and performance of the detector are given in Ref. [15].

3 Monte Carlo simulation

The GEANT4-based [16] Monte Carlo (MC) simulations of e^+e^- annihilations are used to understand the backgrounds and to estimate detection efficiencies. The generator KKMC [17] is used to simulate the e^+e^- annihilation incorporating the effects of the beam-energy spread and initial-state radiation (ISR). The signal modes $\Lambda_c^+ \rightarrow \Sigma^+\eta^{(*)}$ are simulated by taking into account the decay pattern predicted in Ref. [3], in particular the decay asymmetry parameters are used in the simulation. The reference modes $\Lambda_c^+ \rightarrow \Sigma^+\pi^0$ and $\Sigma^+\omega$ are simulated according to the decay patterns observed in data [11]. To study backgrounds, inclusive MC samples consisting of generic $\Lambda_c^+\bar{\Lambda}_c^-$ events, $D_{(s)}^*\bar{D}_{(s)}^{(*)} + X$ production, ISR return to the charmonium(-like) ψ (Y) states at lower masses, and continuum processes $e^+e^- \rightarrow q\bar{q}$ ($q = u, d, s$) are generated, as summarized in Table 1. All decay modes of the Λ_c^+ , ψ and $D_{(s)}$ as specified in the Particle Data Group (PDG) [18] are simulated with the EVTGEN [19] generator, while the unknown decays of the ψ states are generated with LUNDCHARM [20].

Table 1. Summary of the MC samples size for different processes.

process	sample size
$\Lambda_c^+ \rightarrow \Sigma^+\eta$	0.5 M
$\Lambda_c^+ \rightarrow \Sigma^+\eta^{(*)}$	0.5 M
$\Lambda_c^+\bar{\Lambda}_c^-$ (inclusive)	7.75 M
$D_{(s)}^*\bar{D}_{(s)}^{(*)} + X$	10.94 M
ISR	4.0 M
$e^+e^- \rightarrow q\bar{q}$ ($q = u, d, s$)	277.9 M

4 Event selection

In the selection of $\Lambda_c^+ \rightarrow \Sigma^+\eta$, $\Sigma^+\eta'$, $\Sigma^+\pi^0$ and $\Sigma^+\omega$ decays, the intermediate particles Σ^+ , ω and η' are reconstructed in their decays $\Sigma^+ \rightarrow p\pi^0$, $\omega \rightarrow \pi^+\pi^-\pi^0$ and $\eta' \rightarrow \pi^+\pi^-\eta$, while the η and π^0 mesons are reconstructed in their dominant two-photon decay mode.

For each charged track candidate, the polar angle θ in the MDC is required to be in the range $|\cos\theta| < 0.93$. The distances of closest approach to the interaction point are required to be less than 10 cm along the beam direction and less than 1 cm in the plane perpendicular to the beam. The specific ionization energy loss (dE/dx) in the MDC and the time of flight information measured in the TOF are used to calculate particle identification (PID) likelihood values for the pion (\mathcal{L}_π), kaon (\mathcal{L}_K) and proton (\mathcal{L}_p) hypotheses. Pion candidates are selected by requiring $\mathcal{L}_\pi > \mathcal{L}_K$, and proton candidates are required to satisfy

$\mathcal{L}_p > \mathcal{L}_\pi$ and $\mathcal{L}_p > \mathcal{L}_K$.

Photon candidates are reconstructed from isolated clusters in the EMC in the regions $|\cos\theta| \leq 0.80$ (barrel) or $0.86 \leq |\cos\theta| \leq 0.92$ (end-cap). The deposited energy of a cluster is required to be larger than 25 (50) MeV in the barrel (end-cap) region, and the angle between the photon candidate and the nearest charged track must be larger than 10° . To suppress electronic noise and energy deposits unrelated to the events, the difference between the EMC time and the event start time is required to be within (0,700) ns. Candidates for η and π^0 mesons are reconstructed from all $\gamma\gamma$ combinations and the $\gamma\gamma$ invariant mass $M_{\gamma\gamma}$ is required to satisfy $0.50 < M_{\gamma\gamma} < 0.56$ GeV/c² for $\eta \rightarrow \gamma\gamma$, and $0.115 < M_{\gamma\gamma} < 0.150$ GeV/c² for $\pi^0 \rightarrow \gamma\gamma$. A kinematic fit is performed to constrain the $\gamma\gamma$ invariant mass to the nominal mass of η or π^0 [9], and the χ^2 of the kinematic fit is required to be less than 200. The fitted momenta of the η and π^0 are used in the further analysis.

The invariant masses $M_{p\pi^0}$, $M_{\pi^+\pi^-\pi^0}$ and $M_{\pi^+\pi^-\eta}$ are required to be within (1.174, 1.200), (0.760, 0.800) and (0.946, 0.968) GeV/c² for the Σ^+ , ω , and η' candidates, respectively.

The Λ_c^+ candidates for all four decay modes are reconstructed by considering all combinations of selected Σ^+ , ω , π^0 and $\eta^{(\prime)}$ candidates. The Λ_c^+ candidates are identified based on the beam constrained mass, $M_{BC} \equiv \sqrt{E_{beam}^2 - |\vec{p}_{\Lambda_c^+}|^2}$, where E_{beam} is the beam energy and $\vec{p}_{\Lambda_c^+}$

is the momentum of the Λ_c^+ candidate in the rest frame of the initial e^+e^- system. To suppress the combinatorial background, a requirement on the energy difference $\Delta E \equiv E_{beam} - E_{\Lambda_c^+}$ is performed, where $E_{\Lambda_c^+}$ is the energy of the Λ_c^+ candidate. In practice, to improve the resolution of ΔE , a variable $\Delta Q \equiv \Delta E - k \cdot (M_{p\pi^0} - m_{\Sigma^+})$ is defined that decouples the correlation between the measured ΔE and the invariant mass of the Σ^+ candidate, $M_{p\pi^0}$. Here, m_{Σ^+} is the nominal mass of the Σ^+ . The factor k is 1.08 for $\Sigma^+\eta$ and $\Sigma^+\pi^0$, and 0.88 for $\Sigma^+\eta'$ and $\Sigma^+\omega$, as obtained by a fit to the two-dimensional distributions of ΔE versus $M_{p\pi^0}$ with a linear function.

For a specific decay mode, we only keep the candidate with the minimum $|\Delta Q|$ per event. The resultant ΔQ distribution is shown in Fig. 2. A mode-dependent $|\Delta Q|$ requirement, which is approximately three times of its resolution and summarized in Table 2, is applied to select candidate signal events.

To further suppress the combinatorial backgrounds in the $\Lambda_c^+ \rightarrow \Sigma^+\eta$ mode, an anti-proton recoiling against the detected Λ_c^+ candidate is required, which is expected to originate from the $\bar{\Lambda}_c^-$. In order to cancel out systematic uncertainty, the same requirement is applied to the reference mode $\Lambda_c^+ \rightarrow \Sigma^+\pi^0$. For the decay mode $\Lambda_c^+ \rightarrow \Sigma^+\pi^0$, the peaking background from the CF decay mode $\Lambda_c^+ \rightarrow pK_S^0(K_S^0 \rightarrow \pi^0\pi^0)$ is rejected by requiring $M_{\pi^0\pi^0}$ not to be in the range (0.48, 0.52) GeV/c². We also investig-

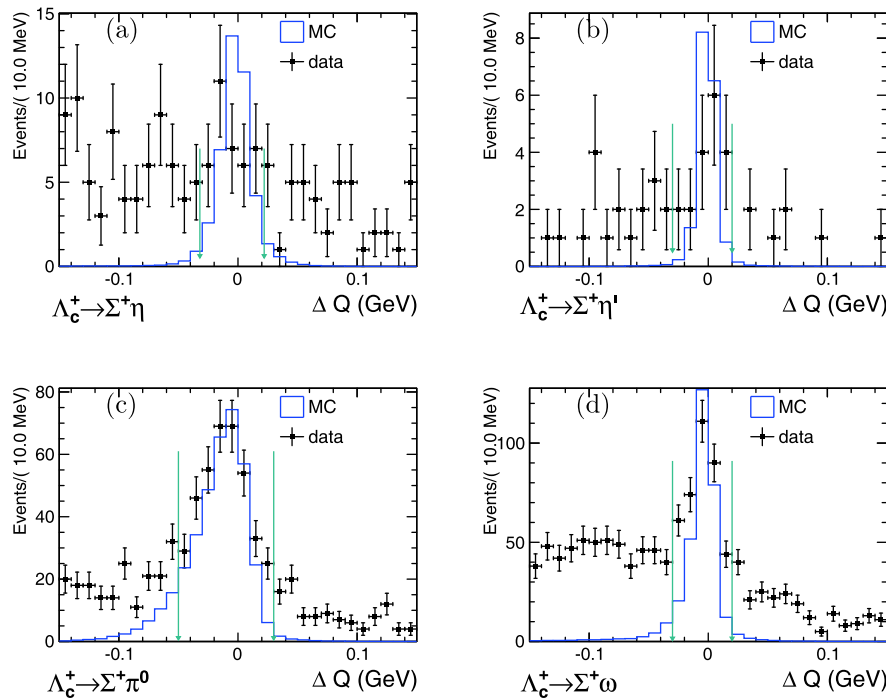


Fig. 2. (color online) Distributions of ΔQ in M_{BC} signal region for $\Lambda_c^+ \rightarrow \Sigma^+\eta$ (a), $\Lambda_c^+ \rightarrow \Sigma^+\eta'$ (b), $\Lambda_c^+ \rightarrow \Sigma^+\pi^0$ (c) and $\Lambda_c^+ \rightarrow \Sigma^+\omega$ (d). Points with error bars are data, solid blue lines are the signal MC samples, the green arrows show the mode-dependent signal region in ΔQ . The signal MC samples are shown with an arbitrary scale to illustrate the signal shape only.

Table 2. Summary of the requirements on ΔQ , signal yields (with statistical uncertainties only) and detection efficiencies for the four decay modes.

decay mode	$\Delta Q/\text{GeV}$	N_i	$\varepsilon_i(\%)$
(a) $\Lambda_c^+ \rightarrow \Sigma^+ \eta$	$[-0.032, 0.022]$	14.6 ± 6.6	7.80
(b) $\Lambda_c^+ \rightarrow \Sigma^+ \eta'$	$[-0.030, 0.020]$	13.0 ± 4.8	4.61
(c) $\Lambda_c^+ \rightarrow \Sigma^+ \pi^0$	$[-0.050, 0.030]$	122.4 ± 14.5	8.98
(d) $\Lambda_c^+ \rightarrow \Sigma^+ \omega$	$[-0.030, 0.020]$	135.4 ± 20.4	7.83

ate the non-resonant background by checking the M_{BC} distribution of events in the sideband region of the Σ^+ , η' and ω invariant mass distribution. No peaking structure from this background is observed.

5 Determination of signal yields

After the application of the above selection criteria, the M_{BC} distributions of the surviving events are depicted in Figs. 3(a) and (b) for the signal decay modes $\Lambda_c^+ \rightarrow \Sigma^+ \eta$ and $\Sigma^+ \eta'$, respectively, and Figs. 3(c) and (d) for the reference decay modes $\Lambda_c^+ \rightarrow \Sigma^+ \pi^0$ and $\Sigma^+ \omega$, respectively. To determine the signal yields, we perform unbinned maximum likelihood fits to the corresponding M_{BC} distributions. In the fit, the signal shapes are described with the MC-simulated signal shapes convolved with a Gaussian function that is used to compensate the resolution difference between data and MC simulations.

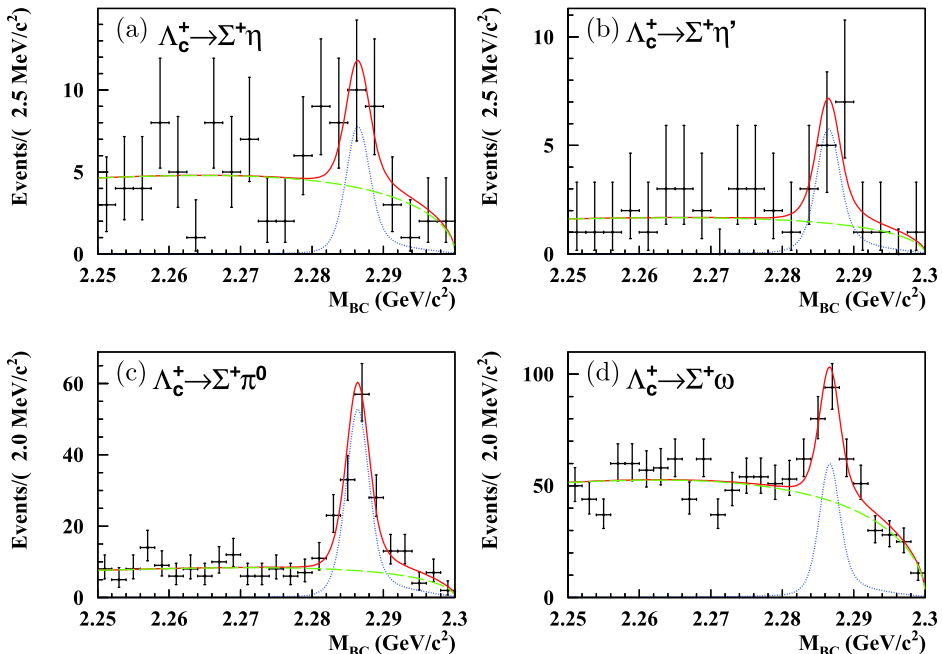


Fig. 3. (color online) Fits to the M_{BC} distributions in data for $\Lambda_c^+ \rightarrow \Sigma^+ \eta$ (a), $\Lambda_c^+ \rightarrow \Sigma^+ \eta'$ (b), $\Lambda_c^+ \rightarrow \Sigma^+ \pi^0$ (c) and $\Lambda_c^+ \rightarrow \Sigma^+ \omega$ (d). Points with error bars are data, solid lines are the sum of the fit functions, dotted lines are signal shapes, long dashed lines are the ARGUS functions.

For the signal decay modes, due to the low statistics, the parameters of the Gaussian functions are constrained to those values obtained by fitting the M_{BC} distributions of the corresponding reference decay modes.

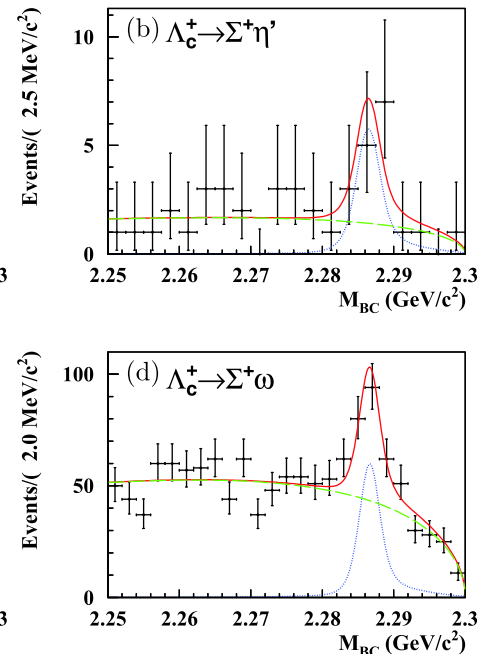
The background shapes are modeled with an ARGUS function [21], fixing the high-end cutoff at E_{beam} . The resulting fit curves are shown in Fig. 3, and the signal yields are listed in Table 2. The relative ratios of BFs between the signal modes and reference modes are calculated with

$$R_{ac} = \frac{\mathcal{B}(a)}{\mathcal{B}(c)} = \frac{N_a \varepsilon_c \mathcal{B}(\pi^0 \rightarrow \gamma\gamma)}{N_c \varepsilon_a \mathcal{B}(\eta \rightarrow \gamma\gamma)}, \quad (1)$$

$$R_{bd} = \frac{\mathcal{B}(b)}{\mathcal{B}(d)} = \frac{N_b \varepsilon_d \mathcal{B}(\omega \rightarrow \pi^+ \pi^- \pi^0) \mathcal{B}(\pi^0 \rightarrow \gamma\gamma)}{N_d \varepsilon_b \mathcal{B}(\eta' \rightarrow \pi^+ \pi^- \eta) \mathcal{B}(\eta \rightarrow \gamma\gamma)}, \quad (2)$$

where the indices a , b , c and d represent the decay modes $\Lambda_c^+ \rightarrow \Sigma^+ \eta$, $\Sigma^+ \eta'$, $\Sigma^+ \pi^0$ and $\Sigma^+ \omega$, respectively. $\mathcal{B}(\pi^0 \rightarrow \gamma\gamma)$, $\mathcal{B}(\eta \rightarrow \gamma\gamma)$, $\mathcal{B}(\eta' \rightarrow \pi^+ \pi^- \eta)$ and $\mathcal{B}(\omega \rightarrow \pi^+ \pi^- \pi^0)$ are the BFs for π^0 , η , η' and ω decays quoted from PDG [9], N_i is the corresponding signal yield and ε_i is the detection efficiency estimated using MC simulations. The signal yields and detection efficiencies of the different decay modes are summarized in Table 2. The resultant ratios are determined to be $R_{ac} = 0.35 \pm 0.16$ and $R_{bd} = 0.86 \pm 0.34$, where the uncertainties are statistical only.

The statistical significance of the signals for $\Lambda_c^+ \rightarrow \Sigma^+ \eta$ and $\Sigma^+ \eta'$ are 2.5σ and 3.2σ , respectively, which are determined by comparing the likelihood values of the fit with and without the signal component and



taking into account the change of the degrees of freedom.

Using the Bayesian method, we set the upper limits at the 90% confidence level (CL) on the signal yields $N_a^{\text{UL}} = 24$, corresponding to a ratio of BFs at the 90% CL $R_{ac} < 0.58$ for the decay $\Lambda_c^+ \rightarrow \Sigma^+ \eta$, and $N_b^{\text{UL}} = 19$ and $R_{bd} < 1.2$ for the decay $\Lambda_c^+ \rightarrow \Sigma^+ \eta'$. The systematic uncertainties discussed below are taken into account by convolving the likelihood curve obtained from the nominal fits with Gaussian functions whose widths represent the systematic uncertainties.

6 Systematic uncertainty

Due to the limited statistics, the total uncertainties are dominated by the statistical errors. The systematic uncertainties associated with Σ^+ detection, tracking and PID of charged pions, and photon selections cancel in the measurement of the ratios of the BFs.

We study the uncertainty associated with the resolution differences between data and MC simulation for η and π^0 invariant mass distributions by smearing the η and π^0 mass distributions of MC samples with a Gaussian function with a width of $2 \text{ MeV}/c^2$, as determined by a study of the control channel $D^0 \rightarrow K^- \pi^+ \pi^0$. The resultant relative changes on the ratios of BFs are 0.3% for R_{ac} and 0.5% for R_{bd} and are taken as the systematic uncertainty due to the different mass resolutions.

We evaluate the uncertainties associated with η' , ω mass requirements and $K_S^0 \rightarrow \pi^0 \pi^0$ veto with analogous method, and the resultant systematics on R_{ac} and R_{bd} are determined to be 0.5% and 0.7%, respectively.

The uncertainty related to the ΔQ requirement is estimated by smearing the ΔQ distributions of MC samples with a Gaussian function with a width of 5 MeV. The corresponding changes, 0.6% for R_{ac} and 0.3% for R_{bd} , are taken as the systematic uncertainties. The uncertainties associated with the fit procedure used to determine the signal yields are studied by performing alternative fits with different fit parameters and fit ranges. More specifically, we vary the values of the two parameters of the Gaussian functions by $\pm 1\sigma$, the ARGUS cut-off by $\pm 5 \text{ MeV}/c^2$ and the fit range by $\pm 10 \text{ MeV}/c^2$. Adding the resultant differences in quadrature, we obtain the systematic uncertainty to be 5.9% and 1.5% for the R_{ac} and R_{bd} , respectively.

The systematic uncertainties associated with the MC modeling that was used to calculate the detection efficiency are evaluated with different signal MC samples. In the nominal analysis, due to limited statistics, the signal MC samples are generated with the helicity angle parameters given in Ref. [3]. We generate an alternative signal MC sample with additional effects on the decay asymmetry with parameter variations of ± 0.2 based on

those in Ref. [3]. The resultant changes in the detection efficiencies, which are 2.6% for R_{ac} and 4.4% for R_{bd} , are taken as the systematic uncertainties.

The uncertainties of the MC statistics and the decay BFs for the intermediate decays ($\mathcal{B}_{\text{inter}}$) quoted from the PDG [9] are also considered. All the individual systematic uncertainties are summarized in Table 3. The total systematic uncertainties for the measurements of R_{ac} and R_{bd} , 6.5% and 5.1%, respectively, are obtained by adding the individual values in quadrature.

Table 3. Summary of the relative systematic uncertainties in the BF ratio measurements (in unit of %).

source	R_{ac}	R_{bd}
$\eta'(\omega)$ mass requirement	–	0.7
$\eta(\pi^0)$ mass requirement	0.3	0.5
ΔQ requirement	0.6	0.3
$\pi^0 \pi^0$ veto	0.5	–
M_{BC} fit	5.9	1.5
MC modeling	2.6	4.4
MC statistics	0.2	0.2
$\mathcal{B}_{\text{inter}}$	0.5	1.9
total	6.5	5.1

7 Summary

In summary, by analyzing a data sample of $e^+ e^-$ collisions corresponding to an integrated luminosity of 567 pb^{-1} taken at a center-of-mass energy of 4.6 GeV with the BESIII detector at the BEPCII collider, we find evidence for the decays $\Lambda_c^+ \rightarrow \Sigma^+ \eta$ and $\Sigma^+ \eta'$ with statistical significance of 2.5σ and 3.2σ . The BFs for $\Lambda_c^+ \rightarrow \Sigma^+ \eta$ and $\Sigma^+ \eta'$ with respect to those of the reference decay modes of $\Lambda_c^+ \rightarrow \Sigma^+ \pi^0$ and $\Sigma^+ \omega$ are $\frac{\mathcal{B}(\Lambda_c^+ \rightarrow \Sigma^+ \eta)}{\mathcal{B}(\Lambda_c^+ \rightarrow \Sigma^+ \pi^0)} = 0.35 \pm 0.16 \pm 0.02$ and $\frac{\mathcal{B}(\Lambda_c^+ \rightarrow \Sigma^+ \eta')}{\mathcal{B}(\Lambda_c^+ \rightarrow \Sigma^+ \omega)} = 0.86 \pm 0.34 \pm 0.04$, respectively. Their 90% CL upper limits are set to be $\frac{\mathcal{B}(\Lambda_c^+ \rightarrow \Sigma^+ \eta)}{\mathcal{B}(\Lambda_c^+ \rightarrow \Sigma^+ \pi^0)} < 0.58$ and $\frac{\mathcal{B}(\Lambda_c^+ \rightarrow \Sigma^+ \eta')}{\mathcal{B}(\Lambda_c^+ \rightarrow \Sigma^+ \omega)} < 1.2$ after taking into account the systematic uncertainties. Incorporating the BESIII results of $\mathcal{B}(\Lambda_c^+ \rightarrow \Sigma^+ \pi^0)$ and $\mathcal{B}(\Lambda_c^+ \rightarrow \Sigma^+ \omega)$ from Ref. [11], we obtain $\mathcal{B}(\Lambda_c^+ \rightarrow \Sigma^+ \eta) = (0.41 \pm 0.19 \pm 0.05)\%$ ($< 0.68\%$), and $\mathcal{B}(\Lambda_c^+ \rightarrow \Sigma^+ \eta') = (1.34 \pm 0.53 \pm 0.19)\%$ ($< 1.9\%$).

Comparisons of the experimental measurements with theoretical predictions from different models are shown in Table 4. The central value of $\mathcal{B}(\Lambda_c^+ \rightarrow \Sigma^+ \eta)$ presented in this work is smaller than that from CLEO [12], while they are compatible within 1σ of uncertainty. The BF of $\Lambda_c^+ \rightarrow \Sigma^+ \eta'$ is measured for the first time, which stands a discrepancy about 2σ of uncertainty from the most of the

Table 4. Comparisons of the measured results with theoretical predictions (in unit of %).

decay mode	körner [5]	sharma [3]	zenczykowski [4]	ivanov [6]	CLEO [12]	this work
$\Lambda_c^+ \rightarrow \Sigma^+ \eta$	0.16	0.57	0.94	0.11	0.70±0.23	0.41±0.20 (<0.68)
$\Lambda_c^+ \rightarrow \Sigma^+ \eta'$	1.28	0.10	0.12	0.12	—	1.34±0.56 (<1.9)

theoretical predictions, but in good agreement with the prediction in Ref. [5]. Furthermore, it is worth noting that the obtained $\mathcal{B}(\Lambda_c^+ \rightarrow \Sigma^+ \eta')$ is larger than $\mathcal{B}(\Lambda_c^+ \rightarrow \Sigma^+ \eta)$, the corresponding ratio is determined to be $\frac{\mathcal{B}(\Lambda_c^+ \rightarrow \Sigma^+ \eta')}{\mathcal{B}(\Lambda_c^+ \rightarrow \Sigma^+ \eta)} = 3.5 \pm 2.1 \pm 0.4$, which contradicts with the

predictions in Refs. [3, 4]. However, the precision of the current results is still poor and further constraints demand improved measurements.

The BESIII collaboration thanks the staff of BEPCII and the IHEP computing center for their strong support.

References

- 1 T. Uppal, R.C. Verma, and M.P. Khana, *Phys. Rev. D*, **49**: 3417 (1994)
- 2 Q. P. Xu and A.N. Kamal, *Phys. Rev. D*, **46**: 270 (1992)
- 3 K. K. Sharma and R.C. Verma, *Eur. Phys. J. C*, **7**: 217 (1999)
- 4 P. Zenczykowski, *Phys. Rev. D*, **50**: 5787 (1994)
- 5 J. G. Körner and M. Krämer, *Z. Phys. C*, **55**: 659 (1992)
- 6 M. A. Ivanov, J. G. Korner, V. E. Lyubovitskij et al, *Phys. Rev. B*, **442**: 435 (1998)
- 7 L. L. Chau, H. Y. Cheng, and B. Tseng, *Phys. Rev. D*, **54**: 2132 (1996)
- 8 G. S. Abrams et al (Mark II Collaboration), *Phys. Rev. Lett.*, **44**: 10 (1980)
- 9 M. Tanabashi et al (Particle Data Group), *Phys. Rev. D*, **98**: 030001 (2018)
- 10 H. Y. Cheng and B. Tseng, *Phys. Rev. D*, **48**: 4188 (1993)
- 11 M. Ablikim et al (BESIII Collaboration), *Phys. Rev. Lett.*, **116**: 052001 (2016)
- 12 R. Ammar et al (CLEO Collaboration), *Phys. Rev. Lett.*, **74**: 3534 (1995)
- 13 M. Ablikim et al (BESIII Collaboration), *Chin. Phys. C*, **39**: 093001 (2015)
- 14 M. Ablikim et al (BESIII Collaboration), *Chin. Phys. C*, **40**: 063001 (2016)
- 15 M. Ablikim et al (BESIII Collaboration), *Nucl. Instrum. Meth. A*, **614**: 345 (2010)
- 16 S. Agostinelli et al (GEANT4 Collaboration), *Nucl. Instrum. Meth. A*, **506**: 250 (2003)
- 17 S. Jadach, B. F. L. Ward, and Z. Was, *Comput. Phys. Commun.*, **130**, 260 (2000); *Phys. Rev. D*, **63**, 113009 (2001)
- 18 K. A. Olive et al [Particle Data Group], *Chin. Phys. C*, **38**, 090001 (2014) and 2015 update
- 19 D. J. Lange, *Nucl. Instrum. Meth. A*, **462**, 152 (2001); R. G. Ping, *Chin. Phys. C*, **32**, 599 (2008)
- 20 J. C. Chen, G. S. Huang, X. R. Qi et al, *Phys. Rev. D*, **62**: 034003 (2000)
- 21 H. Albrecht et al (ARGUS Collaboration), *Phys. Lett. B*, **241**: 278 (1990)